

Ammoniacal Nitrogen Removal via *Dendrocalamus Asper* Biochar-Activated Carbon

Sharifah Nadzirah Wan Hamid^{1*}, Nur Shafiqah Samsudin¹, Siti Kartina Abdul Karim¹, Juferi Idris²

¹Faculty of Applied Sciences, Universiti Teknologi MARA, 94300 Kota Samarahan, Sarawak, Malaysia

²School of Chemical Engineering, Universiti Teknologi MARA, 94300 Kota Samarahan, Sarawak, Malaysia

Citation:

Wan Hamid, S. H., Samsudin, N.S., Abdul Karim, S. K., & Idris, J. (2025). Ammoniacal nitrogen removal via *Dendrocalamus asper* biochar-activated carbon. *Journal of Smart Science and Technology*, 5(2), 129-141.

ARTICLE INFO

Article history:

Received 24 February 2025

Revised 30 July 2025

Accepted 25 August 2025

Published 30 September 2025

Keywords:

biochar
bamboo activated carbon
ammoniacal nitrogen
chemical activation
adsorption capacity
kinetics

DOI:

10.24191/jsst.v5i2.115

ABSTRACT

The porous architecture and series of surface functional groups of bamboo-derived biochar have demonstrated promising potential for flocculation and coagulation in wastewater treatment applications. *Dendrocalamus asper* biochar (pyrolysed at 900 °C in N₂ for 5 hours) was subjected to additional carbonisation and chemically activated with KOH (5:1 w/w) in a furnace at 500 °C for 2 hours to produce activated carbon. The objectives were to determine the optimal mass dosage for ammoniacal nitrogen removal, quantify the adsorption capacity (Q_e, mg g⁻¹), and characterise surface functional groups via Fourier-transform infrared spectroscopy (FTIR). FTIR spectra of treated and untreated biochar revealed O–H stretching, aromatic rings, and C=C alkenes, indicating similar functional profiles. KOH-treated biochar achieved a maximum adsorption capacity of 46.08 mg g⁻¹ versus 44.11 mg g⁻¹ for untreated biochar at an optimal contact time of 143 minutes. Increasing biochar dosage marginally decreased q_e due to competitive adsorption–desorption phenomena, yet enhanced removal efficiency. The treated biochar exhibited only marginal improvements, achieving a 2.85% increase in removal efficiency and a 1.97 mg g⁻¹ increase in adsorption capacity. Kinetic analysis confirmed that ammoniacal nitrogen adsorption adhered to a pseudo-second-order model ($r^2 = 0.9933\text{--}1.000$), with rate constants (k₂) ranging from 1.827×10^7 to 6.5828×10^6 h⁻¹ and modelled q_e between 55.49 and 59.41 mg g⁻¹. The results demonstrate that both treated and untreated bamboo biochars are effective in removing ammoniacal nitrogen with negligible performance disparity. It is suggested to optimise activation parameters, including duration, temperature, and impregnation ratio. Additionally, conducting proximate or ultimate analysis, measuring the BET surface area, and performing SEM characterisation are recommended for a comprehensive evaluation.

* Corresponding author. E-mail address: shnadzirah@uitm.edu.my

<https://doi.org/10.24191/jsst.v5i2.115>



© 2025 by the authors. Submitted for possible open access publication under the terms and conditions of the Creative Commons Attribution (CC BY) license (<http://creativecommons.org/licenses/by/4.0/>).

1 INTRODUCTION

Excessive industrialisation has increased water, air, and land pollution, creating environmental and health risks. Biochar, an innovative sorbent, offers benefits such as a diverse feedstock source, simple synthesis, and excellent structural characteristics¹. Despite persistent environmental pressures, future research should prioritise the development and optimisation of biochar-based strategies for effective water and wastewater treatment. Ammoniacal nitrogen in industrial and agricultural effluents poses significant ecological risks and threats to human health. Activated carbon produced from bamboo biochar improves filtration performance while preventing the formation of harmful byproducts². Biochar has a lower environmental impact than activated carbon and may be more cost-effective in terms of functionality³. Recently, there has been significant growth in the investigation of contaminants' adsorption and sewage purification using biochar⁴.

The biochar's porous physical features enable it to attach easily with other substances, and its firm structure allows it to exist for a long time⁵. Recent advancements in biochar technology have identified *Dendrocalamus asper* biochar-derived activated carbon as a promising material for remediation. Produced via optimised pyrolysis and subsequent chemical activation, this adsorbent exhibits porosity and abundant functional groups, enabling efficient adsorption of ammoniacal nitrogen. These qualities have led to the assumption that biochar offers several benefits for both agriculture and water quality. These pros include improved soil moisture retention. This benefits plant development in low-nutrient soils⁶. This improves water quality by reducing nitrogen leaching into groundwater and discharging into surface water⁷. Therefore, biochar can stabilise carbon storage⁸. It offers a technique for sequestering carbon from different organic wastes rather than releasing carbon into the atmosphere through regular burning⁹.

Furthermore, biochar possesses a highly adsorbent surface with numerous functional groups, allowing it to absorb and filter contaminants, such as metals, from water¹⁰. As a result, biochar has also been employed successfully in the wastewater treatment process. Moreover, bamboo biochar has significant benefits. It is a stable, carbon-dense solid that may last in soil for centuries, exhibiting resistance to decomposition¹¹. In addition, its porosity is substantially larger than that of hardwood charcoal, showing twice the absorption efficiency¹². The higher carbon content makes it an exceptional reservoir for carbon storage in soil development¹³. The production of bamboo biochar through a pyrolysis method stabilises carbon from biomass and contributes to long-term carbon sequestration^{4,11}. These characteristics enhance its utility not only in wastewater remediation but also in improving soil quality.

Incorporating bamboo biochar in agriculture increases soil moisture retention and nutrient availability, thereby leading to enhanced plant productivity and reduced nutrient leaching^{12,14}. It can boost agricultural yields by 50-70% by absorbing and retaining moisture, nutrients, fertilisers, and soil microorganisms, while neutralising acidic soils and recovering damaged lands¹⁴. It promotes plant development, feeds soil microbial populations and optimises water management¹². In addition to its agricultural benefits, bamboo biochar reduces undesirable odours, purifies the air, regulates humidity, absorbs electromagnetic radiation, and improves human health¹⁵. It is also used to manufacture activated carbon, which is characterised by porosity and is ideal for the treatment of air, water, and wastewater^{2,11}. Hence, this research aims to analyse the optimal mass dosage of *Dendrocalamus asper* activated carbon to assess its effectiveness in removing ammoniacal nitrogen, its adsorption capacity, and the properties of surface functional groups in the upper nodes and lower nodes of bamboo biochar. This study determines whether there is a significant difference in the samples.

2 MATERIAL AND METHODS

The materials and chemicals used include bamboo biochar, 25 mL potassium hydroxide (85% volume solution), hydrochloric acid, deionised water, beaker, mortar, anhydrous ammonium nitrate (Bendosen), Rochelle Salt (Potassium Sodium Tartarate from Bendosen), and Nessler's reagent (Hach).

2.1 Sample collection

Bamboo *Dendrocalamus asper* biochar was collected from ANT Supplies Sdn. Bhd.

2.2 Preparation and treatment of bamboo biochar activated carbon

The original untreated form of bamboo biochar (pyrolysed with nitrogen gas at 900 °C for 5 hours) was collected from Ant Supplies Sdn. Bhd. The bamboo biochar was further crushed into a fine powder. The biochar was placed in a 1000 mL beaker. The impregnation volume ratio of the treatment was 5:1. The ratio of concentrated potassium hydroxide was 5, whereas the ratio of biochar was 1. Consequently, it was left in the oven for 24 hours. The biochar was impregnated with potassium hydroxide for 24 hours to initiate the treatment activation using the muffler furnace at 500 °C for 2 hours. The treated activated biochar was washed with hydrochloric acid until the pH reached 7. The filtered biochar was dried in the oven for 48 hours until it reached a constant mass.

2.3 Characterisation of bamboo biochar activated carbon

For FTIR analysis, the bamboo biochar samples were divided into four parts of nodes (segments) cut from the bamboo culm (upper node of treated bamboo biochar, upper node of untreated bamboo biochar, lower node of treated bamboo biochar, and lower node of untreated bamboo biochar) to examine the difference in surface functional groups between the nodes. The four samples were crushed into fine powder, and 1 mg of biochar was used for each. As the samples were in fine powder form, they could easily be analysed using an attenuated total reflectance (ATR) accessory, allowing immediate measurement without extensive preparation. The first step was to clean the ATR crystal with ethanol to eliminate contaminants. Then, 1 mg of fine powder was added to each sample and placed directly on the ATR crystal. Subsequently, pressure was applied using the ATR pressure clamp to ensure optimal contact between the sample and the crystal. The FTIR analysis was performed over a wavenumber range from 4000 cm^{-1} to 500 cm^{-1} with a resolution of 4 cm^{-1} . Each sample was scanned 8 times. Afterwards, the FTIR scan was initiated. FTIR analyses were conducted on treated and untreated samples to identify the surface functional groups of biochar using the FTIR instrument (L1600107 PerkinElmer), under controlled room temperature and humidity conditions.

2.4 Standard solution of ammoniacal nitrogen preparation

An ammonium standard was prepared by dissolving 3.819 g of anhydrous ammonium nitrate in 1000 mL of deionised water. Any ammonia content in the deionised water was eliminated by boiling 50 g of Rochelle salt solution with 100 mL of deionised water. The ammonium standard was prepared using stock solutions of 10, 20, 30, 40, and 50 mg L^{-1} , corresponding to 10, 20, 30, 40, and 50 mL of ammonium nitrate solution, respectively respectively¹⁶. Following a five-minute interval, 1 mL of Rochelle salt solution and 1 mL of Nessler's reagent were added. The diluted solutions of ammoniacal nitrogen concentrations were suitably produced for the subsequent batch of adsorption processes. The concentration of ammoniacal nitrogen was determined using a UV-Vis Spectrophotometer (Thermo SCIENTIFIC GENESYS 20). Initially, ensure that the sample is clear and free of particles. The instrument was turned on and warmed up for 10-15 minutes. The wavelength was set at 425 nm. Subsequently, the standard and the sample were filled into separate plastic cuvettes. Then, they were placed in the sample holder, keeping the same orientation as the blank. The readings of each sample were recorded. Following data collection and analysis, proper cleaning and shutdown procedures were conducted to ensure the instrument's precision and durability.

2.5 Preparation of batch experiment

In various conical flasks, 0.05 g of biochar was mixed with 50 mL of ammoniacal nitrogen solutions of fixed concentration. The mixtures were stirred at 150 rpm for 300 minutes¹⁷ at a room temperature of

25 °C (298 K). Using the provided equation 1 and 2, the quantity of ammoniacal nitrogen adsorbed, q_e (mg g⁻¹), and percentage of removal were determined:

$$q_e = (C_i - C_e)V/m \quad (1)$$

q_e = equilibrium capacity (mg g⁻¹)

V = Volume of ammoniacal nitrogen solution (mL)

m = Mass of activated carbon (g)

C_i = Initial concentration of ammoniacal nitrogen (mg L⁻¹)

C_f = Final (equilibrium) concentration of ammoniacal nitrogen (mg L⁻¹)

$$\text{Percentage of removal;} = \frac{\text{Initial} - \text{Final}}{\text{Initial}} \times 100 \quad (2)$$

Initial = Initial measurement before treatment of wastewater

Final = Final measurement after treatment of wastewater

2.6 The effect of mass sample dosage

The effects of adsorbent dosage were analysed by mixing 50 mL of 50 ppm ammoniacal nitrogen solutions of constant concentration with 0.005, 0.01, and 0.05 g of biochar, held for 300 minutes at a stirring rate of 150 rpm¹⁷ at 298 K.

2.7 Kinetic studies

A kinetic study was conducted using 0.05 g of *Dendrocalamus asper* biochar (based on the optimum mass dosage in 2.6) in a 50 ppm NH₄-N solution. The final concentrations of the kinetic model were measured at 15, 30, 60, 90, 135, 180, 225, 270, and 300 minutes and were determined using a UV-Vis Spectrophotometer at 425 nm. Initially, it is crucial to ensure that the sample is clear and free of particles. To set up the instrument, the spectrophotometer was turned on and allowed to warm up for 10-15 minutes. The wavelength was set at 425 nm. The plastic cuvette was filled with the solvent, and the blank was placed into the sample holder of the spectrophotometer. A blank scan was conducted to calibrate the instrument to zero. After that, a clean cuvette was filled with the prepared sample, and the outside of the cuvette was cleaned with a tissue to remove smudges. The cuvette was placed into the sample holder in the same orientation as the blank. The readings of each sample were recorded. Following data collection and analysis, proper cleaning and shutdown procedures were conducted to ensure the instrument's precision and durability. Hence, the kinetic model was determined for *Dendrocalamus asper* activated carbon.

3 FINDINGS AND DISCUSSION

3.1 Characteristics of bamboo biochar and bamboo activated carbon

Fig. 1 illustrates the FTIR spectra of biochar, untreated and after KOH treatment, for both the upper node of bamboo biochar and the lower node of bamboo biochar samples. In Fig. 1, the only difference observed after treatment is that the upper untreated sample of bamboo biochar exhibits greater intensity than the upper treated sample at a peak of 1746 cm⁻¹, attributed to the significant stretching of C-H bonds¹⁸. Table 1 summarises the surface functional groups on both untreated and KOH-treated surfaces. The C-H bending, C=C alkene, O-H alcohols, and aromatic rings remain invariant in treated and untreated biochar. In Fig. 1, the lower treated and untreated samples reveal a notable difference in surface functional groups. A peak emerges at 700 cm⁻¹, shifting from 873 cm⁻¹, ascribed to C=C bending. The peak at 1040 cm⁻¹ likely corresponds to C-OH bonding, exhibiting substantially more vigorous stretching than the lower treatment, which registers at 963 cm⁻¹.

Furthermore, the C-H broadband peak seen in the untreated sample at 1463 cm⁻¹ suggests the existence of several shoulders and minor bands, resulting in a greater intensity than the treated sample. The

transition from 1872 cm^{-1} to 1445 cm^{-1} indicates weak to medium C-H bending. Overall, the treated and untreated upper and lower nodes of bamboo biochar did not show a significant difference in the surface functional group, as they both possessed similar functional groups.

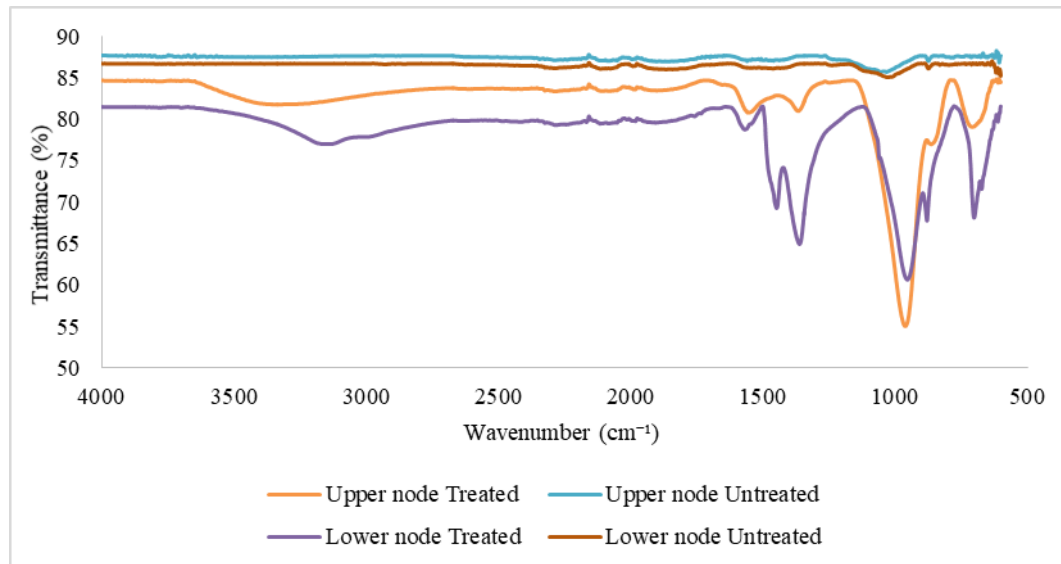


Fig. 1. FTIR analysis of the functional groups of biochar samples before and after treatment.

Table 1: Surface functional group of untreated and treated bamboo biochar

Functional group (Vibration type)	Wavenumber (cm^{-1})		Composition	Significance in adsorption
	Untreated	Treated		
C-H (Bending)	1445		Aliphatic compounds	Adsorbs non-polar compounds via hydrophobic forces
Carbonyl (C=O) (Stretching)	1872	1746	Organic compounds	Adsorbs polar compounds via hydrogen bonding
CH ₂ (Bending)	1463	1368	Aliphatic compounds	Adsorbs non-polar compounds (untreated) / van der Waals forces (treated)
Aromatic C-H (stretching)	873	700	Aromatic compounds	Adsorbs aromatic compounds via π - π interactions
Aromatic C-H (Deformation)		788	Aromatic compounds	Enhances adsorption through π - π stacking
C-O (Stretching)	963	1040	Oxygenated organic compounds	Adsorbs metal ions and polar molecules
C=C (Aromatic Stretch)	1599	1559	Aromatic compounds	Enhances adsorption with aromatic adsorbates (untreated) / Adsorbs aromatic species via π - π interactions (treated)

3.2 Adsorption studies

Fig. 2 shows that after about 143 minutes, the graph exhibited a smaller gradient, indicating that the adsorption capacity of ammoniacal nitrogen augmented with prolonged contact time until it approached near saturation at 300 minutes.

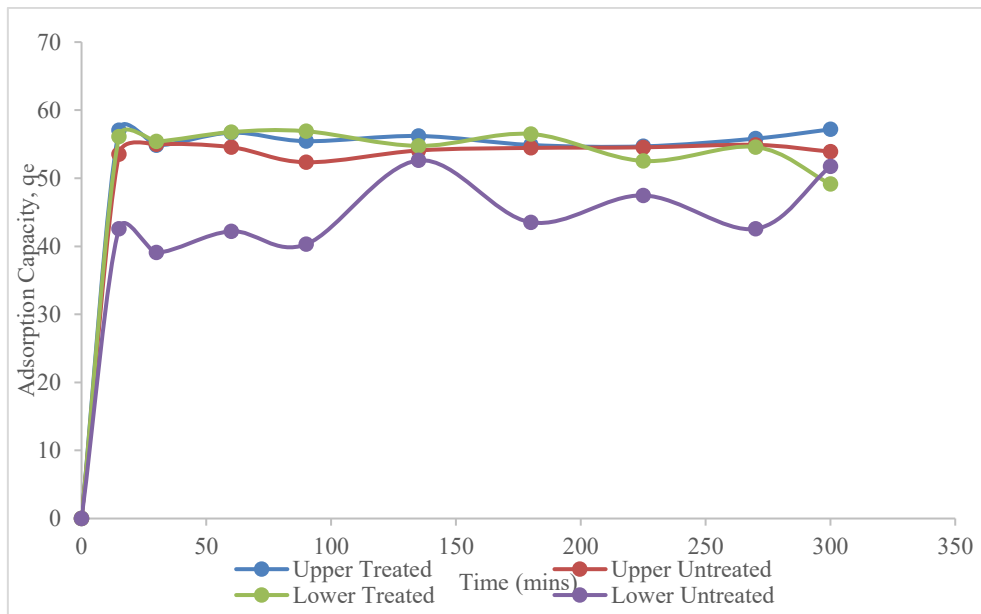


Fig. 2. The effect of shaking/contact time versus ammoniacal nitrogen removal by biochar samples at 0.04 g, 50 ppm, 150 rpm, and 300 minutes.

Table 2 show the impact of adsorbent dose on the adsorption of ammoniacal nitrogen by both treated and untreated biochar samples. The data presented in the tables reveal that an increase in mass dosage corresponds with enhanced removal effectiveness, though the differences are minimal. The adsorbent's growth enhances the availability of potential adsorptive sites. The 0.05 g dosage has the highest removal percentage for both treated (92.19%) and untreated (89.34%), with the adsorption capacity of 46.08 mg g^{-1} (treated) and 44.11 mg g^{-1} (untreated). The difference of 2.85% removal percentage and 1.97 mg g^{-1} in adsorption capacity is considered low. The low differences between treated and untreated biochar are because pyrolysis of the untreated biochar at high temperature (900°C) already induces structural maturity, where it undergoes extensive devolatilisation, aromatisation, and micropore formation. The high-temperature carbonisation yields a carbon-rich matrix with stable surface chemistry and hierarchical pore structures, which are often sufficient for ammonium adsorption without further activation¹⁹. Secondly, the limited KOH activation temperature of 500°C post-pyrolysis may be thermally insufficient to fully mobilise potassium ions for effective pore development or surface etching. Previous studies indicate KOH activation is most effective at temperatures $\geq 700^\circ\text{C}$, where intercalation and chemical activation significantly alter surface area and microporosity^{20,21}, resulting in a slight difference in percentage removal and adsorption capacity. Thirdly, the dominance of surface functional groups over textural effects suggests that treated and untreated biochars retain essential oxygenated groups such as $-\text{OH}$ and $\text{C}=\text{O}$ that govern ammonium adsorption via ion exchange and electrostatic interactions. Since these groups are already abundant from raw biomass or pyrolysis, the surface functional group chemistry is likely the key contributor at low dosages, hence not the pore volume^{22,23}. Lastly, due to the active site efficiency at 0.05 g dosage, surface active sites are maximally used under unsaturated conditions. The ammonium concentration per gram of biochar is high, even marginal differences in surface area or pore structure become less impactful than surface chemistry and accessibility²⁴.

The decrease trend and the increase trend are due to the desorption. Desorption of ammoniacal nitrogen can result from weak physical forces where the adsorbate interacts with the adsorbent through van der Waals forces. These interactions are generally less stable and more prone to disruption under variable environmental conditions^{3,25}. Additionally, desorption may occur when the adsorption sites become saturated. In this situation, incoming ammoniacal nitrogen molecules displace those previously adsorbed

due to competitive binding²⁶. Furthermore, some adsorption processes are deliberately reversible, allowing for the desorption of adsorbed molecules to recover the adsorbate or regenerate the adsorbent for reuse²⁷. These factors underline the dynamic equilibrium in adsorption-desorption systems, highlighting the need for optimised experimental conditions to minimise desorption and enhance the adsorption process²⁸.

Table 2: Effect of adsorbent dosage on percentage removal and amount of ammoniacal nitrogen adsorbed at equilibrium on ammoniacal nitrogen by biochar samples (Upper and lower nodes mixture of treated and untreated bamboo biochar)

Dosage (g)	Removal (%)		Adsorption Capacity, q_e (mg/g)	
	Treated	Untreated	Treated	Untreated
0.005	91.76	88.96	45.88	44.35
0.01	92.15	89.30	23.02	22.16
0.05	92.19	89.34	46.08	44.11

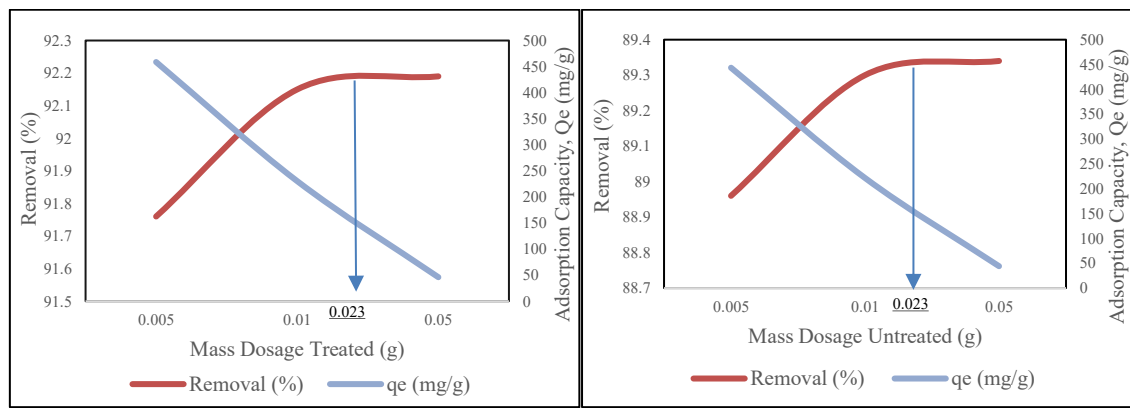


Fig. 3. Adsorbent dosage effect on ammoniacal nitrogen adsorption by (a) treated and (b) untreated biochar activated carbon.

The adsorption capacity observed in this study exhibited a slight difference of 0.2 g for treated biochar and 1.77 g for untreated biochar at a mass dosage of 0.05 g. Fig. 3 illustrates the percentage removal of ammoniacal nitrogen plotted against mass dosage on the primary axis. In contrast, the adsorption capacity of ammoniacal nitrogen relative to dosage is represented on the secondary axis. According to Fig. 3, as the dosage of treated biochar increased, the adsorption capacity gradually decreased. On the contrary, the removal efficiency improved over time and stabilised once the treated biochar dosage reached 0.023 g. The equilibrium adsorption capacity declined with increasing treated biochar dosage due to the aggregation of adsorption sites and a corresponding decrease in the adsorption area. The slight difference in removal and adsorption capacity (2.85% and 1.97 mg g⁻¹) in ammoniacal nitrogen removal between treated and untreated biochar is minimal since both treated and untreated biochar already showed good removal efficiency. In contrast, the treated activated biochar did not substantially improve the ammoniacal adsorption in this analysis compared to the cost, process, and time required for the bamboo biochar.

Table 3 presents the quantity of NH₄-N adsorbed at equilibrium (q_e), the slope and intercept, and the kinetic models' rate constants (k_1 and k_2). The initial adsorbed quantity (h) was computed in the table. The computed range for the constant rate (k_1) of the pseudo-first-order kinetics is 0.0065-0.3926 h⁻¹, and for q_e , it is 1.5012-55.1634 mg g⁻¹ with correlation coefficient values ranging from 0.0447 to 0.9585. The pseudo-second-order model indicated that the ranges for the rate constant (k_2) and q_e are 1.824x10⁻⁷ to 6.5828x10⁻⁶ and 52.3560 to 64.5161 mg g⁻¹, respectively, with correlation coefficients ranging from 0.9933

to 1.000 (Table 3). The correlation of the pseudo-second-order model surpassed that of the pseudo-first-order model. The adsorption of NH₄-N seems to align more closely with the pseudo-second-order model across all samples.

Table 3: Parameters calculated for the pseudo-first and second-order model from kinetic models

Sample	Pseudo-first Order			Pseudo-Second Order			q _e (exp)	
	k ₁	q _e	r ²	k ₂	h	q _e		
Lower treated	0.3926	55.1634	0.9585	6.5828 × 10 ⁻⁶	0.0274	64.5161	0.9933	56.4134
Lower untreated	0.0065	1.8349	0.0071	1.9992 × 10 ⁻⁷	0.0007	59.1716	0.9999	59.4082
Upper treated	0.0643	1.5012	0.8987	2.5347 × 10 ⁻⁷	0.0008	56.1798	1.000	56.7031
Lower untreated	0.0246	3.9789	0.0447	1.824 × 10 ⁻⁷	0.0005	52.3560	0.9981	55.4922

*¹k₁: Pseudo-first kinetic constant of NH₄-N, ²q_e: Adsorption amount from pseudo-first-order equation, ³q_e(exp): Adsorption amount from experiment data

The adsorption study on the removal of ammoniacal nitrogen has shown minor differences in the adsorption and kinetic study. The removal and adsorption capacity only showed 2.85% and 1.97 mg g⁻¹ differences. The slight differences in removal percentage and equilibrium adsorption capacity (q_e) between treated and untreated biochar can arise due to numerous factors, such as existing untreated biochar structural maturity, inefficient chemical treatment, dominance of surface functional groups, and active site efficiency. For the kinetic study, the correlation coefficient (r²) indicated model fit, with optimal kinetic models determined by linear regression and q_e values²⁹. The pseudo-first-order rate constant (k₁) ranged from 0.0643 to 0.3926 h⁻¹, with q_e values of 1.5012–55.1643 mg g⁻¹ (r²: 0.0071–0.9585). The pseudo-second-order model showed k₂ values of 1.827×10⁻⁷ to 6.5828×10⁻⁶ h⁻¹ and q_e values of 52.3560 – 64.5161 mg g⁻¹ (r²: 0.9933–1.000), with the upper treated bamboo biochar having an r² value of 1.000. Higher r² values for the pseudo-second-order model suggest NH₄⁺-N adsorption occurred primarily via chemisorption, which involves chemical interactions such as covalent bonding, governing the process and influencing adsorption rates by active site availability.

The adsorption kinetics of NH₄⁺-N were evaluated using pseudo-first-order and pseudo-second-order models (Fig. 4 and Fig. 5). The pseudo-first-order plots (Fig. 4) displayed poor linearity for most samples, particularly for the untreated types, suggesting limited applicability of this model to describe the adsorption process. Treated adsorbents exhibited slightly better correlation, indicating improved kinetic behaviour after treatment. In contrast, the pseudo-second-order model (Fig. 5) showed excellent linearity across all sample types, with higher correlation coefficients and better conformity to experimental data, implying that chemisorption is the predominant mechanism governing NH₄⁺-N adsorption. Notably, the treated adsorbents, especially the lower treated sample, exhibited steeper slopes, reflecting faster adsorption rates and potentially greater adsorption capacity. These results confirm that surface treatment enhances the adsorptive performance and that the pseudo-second-order model provides a more accurate representation of the adsorption kinetics.

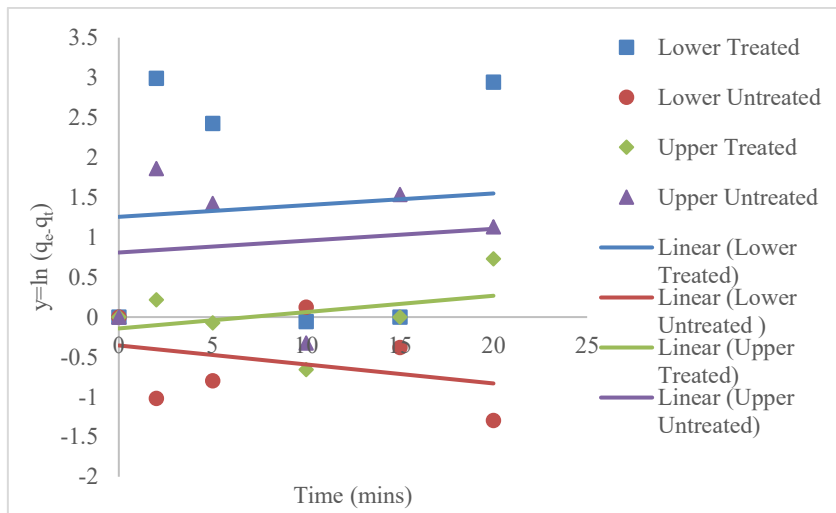


Fig. 4. Pseudo-first-order kinetic plots of NH₄-H on different types (q_e is the adsorption amount at equilibrium (mg g⁻¹), and q_t is the adsorption amount at time t (mg g⁻¹).

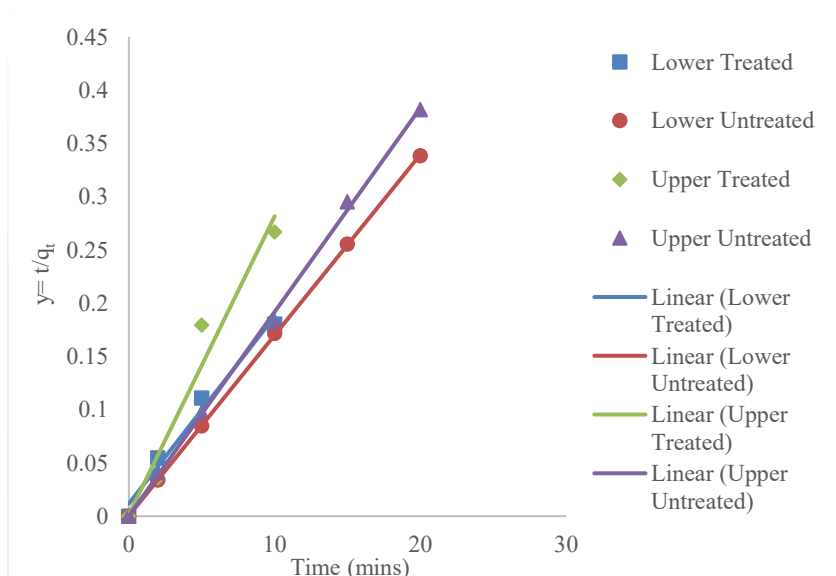


Fig. 5. Pseudo-second-order kinetic plots of NH₄-H on different types (q_e is the adsorption amount at equilibrium (mg g⁻¹), and q_t is the adsorption amount at time t (mg g⁻¹).

The model effectively predicted adsorption behaviour from initial contact to equilibrium, supporting its applicability for system design and scaling³⁰. The strong agreement between experimental and modelled q_e values further validates the reliability of the kinetic framework for performance assessment. Table 4 compares this study and previous similar studies to improve the understanding of bamboo biochar and its activation treatment to advance the adsorption of ammoniacal nitrogen for bamboo biochar.

Table 4. Adsorption characteristics of various contaminants with biochar

Feedstock Activated Carbon	Carbonisation Condition	Activating Agent	BET Surface Area (m ² g ⁻¹)	Adsorption Dosage (g L ⁻¹)	q _e (mg g ⁻¹)	Kinetic Model	References
Lignin removed Moso bamboo	500 °C in N ₂	ZnCl ₂ (1:3)	1580	-	37.2	PFO & PSO	Yuan et al. ³¹
Bamboo sawdust derived biochar	750 °C in N ₂	-	2.5	0.2	0.84	-	Chen et al. ³²
Bamboo derived biochar	370 °C in N ₂	-	229.46	1	11.52	-	Fan et al. ³³
Bamboo biochar montmorillonitec omposite	400 °C in N ₂	-	19.93	0.5	12.52	PSO	Chen et al. ³⁴
Bamboo biochar (<i>Dendrocalamus asper</i>)	900 °C for 5 hours in N ₂	None (biochar)	-	0.05	44.11	PSO	This study
Bamboo biochar (<i>Dendrocalamus asper</i>)	900 °C for 5 hours in N ₂	KOH for another 2 hours	-	0.05	46.08	PSO	This study

Note: All contain ammoniacal nitrogen as contaminants

4 CONCLUSION

This study demonstrates that *Dendrocalamus asper* derived biochar effectively adsorbs ammoniacal nitrogen from aqueous solutions. Fourier-transform infrared spectroscopy (FTIR) revealed that KOH activation marginally enhanced surface functional groups—specifically O–H alcohols, aromatic rings, and C=C alkenes—relative to the untreated material. Under an optimal contact time of 143 minutes, the treated biochar achieved a maximum adsorption capacity (q_e) of 46.08 mg g⁻¹, compared with 44.11 mg g⁻¹ for the untreated sample with 0.05 g mass used. Although higher biochar dosages reduced q_e due to competitive adsorption–desorption dynamics, removal efficiency increased and plateaued at a dosage of 0.023 g. Kinetic modelling confirmed that NH₄⁺–N uptake conforms to a pseudo-second-order mechanism (*r*² = 0.9933–1.000), indicating chemisorption as the rate-limiting step. Rate constants (k₂) ranged from 1.83 × 10⁷ to 6.58 × 10⁶ h⁻¹, yielding modelled q_e values between 52.36 and 64.52 mg g⁻¹. The similarity of experimental mean q_e for treated (56.56 mg g⁻¹) and untreated (57.45 mg g⁻¹) biochars suggests that chemical activation confers only marginal performance gains. Overall, both untreated and treated *Dendrocalamus asper* biochars are validated as efficient, low-cost adsorbents for ammoniacal nitrogen removal although the treated biochar exhibited only marginal improvements over the untreated sample, achieving a 2.85% increase in removal efficiency and a 1.97 mg g⁻¹ increase in adsorption capacity. To further enhance adsorption capacity, future work should optimise activation parameters such as impregnation ratio, temperature, and activation time, by employing proximate and ultimate analyses, Brunauer–Emmett–Teller surface area measurements, and scanning electron microscopy (SEM) for comprehensive material characterisation.

ACKNOWLEDGEMENTS/ FUNDING

The authors would like to acknowledge the support of the Faculty of Applied Sciences, Universiti Teknologi MARA, Cawangan Sarawak, Kampus Samarahan 2 staff and members for the analytical laboratory facilities and excellent technical support towards this research. The authors extend their appreciation to our grant provider, Ant Supply Sdn. Bhd. is responsible for financial and material support during the studies.

CONFLICT OF INTEREST

The authors agree that this research was conducted in the absence of any self-benefits, commercial or financial conflicts and declare the absence of conflicting interests with the funders. The authors agree that this research was conducted in the absence of any self-benefits, commercial or financial conflicts and declare the absence of conflicting interests with the funders.

AUTHORS' CONTRIBUTIONS

Conceptualization: S.N. Wan Hamid, S.K. Abdul Karim, & N.S. Samsudin

Data curation: S.N. Wan Hamid, & N.S. Samsudin

Methodology: S.N. Wan Hamid, S.K. Abdul Karim, & N.S. Samsudin

Formal analysis: S.N. Wan Hamid, S.K. Abdul Karim, & N.S. Samsudin

Visualisation: S.N. Wan Hamid, N.S. Samsudin & J. Idris

Software: S.N. Wan Hamid, & N.S. Samsudin

Writing (original draft): S.N. Wan Hamid, S.K. Abdul Karim, & N.S. Samsudin

Writing (review and editing): S.N. Wan Hamid, S.K. Abdul Karim, N.S. Samsudin & J. Idris

Validation: S.N. Wan Hamid & S.K. Abdul Karim,

Supervision: S.N. Wan Hamid, S.K. Abdul Karim, & J. Idris

Funding acquisition: J. Idris & S.N. Wan Hamid

Project administration: Not available

REFERENCES

1. Wang, X., Cheng, H., Ye, G., Fan, J., Yao, F., Wang, Y., Jiao, Y., Zhu, W., Huang, H., & Ye, D. (2022). Key factors and primary modification methods of activated carbon and their application in adsorption of carbon-based gases: A review. *Chemosphere*, 287(2), 131995. <https://doi.org/10.1016/j.chemosphere.2021.131995>
2. Khuong, D. A., Nguyen, H. N., & Tsubota, T. (2021). Activated carbon produced from bamboo and solid residue by CO₂ activation utilized as CO₂ adsorbents. *Biomass and Bioenergy*, 148, 106039. <https://doi.org/10.1016/j.biombioe.2021.106039>
3. Ambaye, T. G., Vaccari, M., van Hullebusch, E. D., Amrane, A., & Rtimi, S. (2021). Mechanisms and adsorption capacities of biochar for the removal of organic and inorganic pollutants from industrial wastewater. *International Journal of Environmental Science and Technology*, 18, 3273–3294. <https://doi.org/10.1007/s13762-020-03060-w>
4. Alshehri, M. A., & Pugazhendhi, A. (2024). Biochar for wastewater treatment: Addressing contaminants and enhancing sustainability: Challenges and solutions. *Journal of Hazardous Materials Advances*, 16, 100504. <https://doi.org/10.1016/j.hazadv.2024.100504>
5. Yaashikaa, P. R., Kumar, P. S., Varjani, S., & Saravanan, A. (2020). A critical review on the biochar production techniques, characterization, stability and applications for circular bioeconomy. *Biotechnology Reports*, 28, e00570. <https://doi.org/10.1016/j.btre.2020.e00570>
6. Mohubedu, R. P., Diagboya, P. N. E., Abasi, C. Y., Dikio, E. D., & Mtunzi, F. (2019). Magnetic valorization of biomass and biochar of a typical plant nuisance for toxic metals contaminated water treatment. *Journal of Cleaner Production*, 209, 1016–1024. <https://doi.org/10.1016/j.jclepro.2018.10.215>
7. Craswell, E. (2021). Fertilizers and nitrate pollution of surface and ground water: An increasingly pervasive global problem. *SN Applied Sciences*, 3(4), 518. <https://doi.org/10.1007/s42452-021-04521-8>

8. Gross, A., Bromm, T., & Glaser, B. (2021). Soil organic carbon sequestration after biochar application: A global meta-analysis. *Agronomy*, 11(12), 2474. <https://doi.org/10.3390/agronomy11122474>
9. Kowalska, A., Pawlewicz, A., Dusza, M., Jaskulak, M., & Grobelak, A. (2020). Plant–soil interactions in soil organic carbon sequestration as a restoration tool. In M. N. V. Prasad & M. Pietrzykowski (Eds.), *Climate change and soil interactions*, (pp. 663–688). Elsevier. <https://doi.org/10.1016/B978-0-12-818032-7.00023-0>
10. Jagadeesh, N., & Sundaram, B. (2023). Adsorption of Pollutants from Wastewater by Biochar: A Review. *Journal of Hazardous Materials Advances*, 9, 100226. <https://doi.org/10.1016/j.hazadv.2022.100226>
11. Kumar, T., Ansari, S. A., Sawarkar, R., Agashe, A., Singh, L., & Nidheesh, P. V. (2025). Bamboo biochar: a multifunctional material for environmental sustainability. *Biomass Conversion and Biorefinery*, 1-25. <https://doi.org/10.1007/s13399-025-06608-3>
12. Alves, K.S., Guimarães, T., de Carvalho Bittencourt, R. et al. (2025). Bamboo-derived biochars: physicochemical properties and implications for soil fertility and sustainability. *Biomass Conv. Bioref.* 15, 21085–21105 (2025). <https://doi.org/10.1007/s13399-025-06702-6>
13. Basile-Doelsch, I., Balesdent, J., & Pellerin, S. (2020). Reviews and syntheses: The mechanisms underlying carbon storage in soil. *Biogeosciences*, 17(21), 5223–5242. <https://doi.org/10.5194/bg-17-5223-2020>
14. Alfei, S., & Pandoli, O. G. (2024). Bamboo-based biochar: A still too little-studied black gold and its current applications. *Journal of Xenobiotics*, 14(1), 416–451. <https://doi.org/10.3390/jox14010026>
15. Jos, S., Mohidin, H., Ahmed, O. H., Kassim, N. Q. B., Mahdian, S., & Rosli, N. (2024). Mitigating Nitrogen Leaching in Mineral Soils using Pineapple Leaf Biochar. *Malaysian Journal of Soil Science*, 28. Retrieve from: https://msss.com.my/mjss/Full%20Text/vol28/V28_01.pdf
16. Wylie, D. A. (2025). *Application of Modified Flax Fibres as Bio-Sorbents for the Removal of Ammonia from Liquid Phase* (Doctoral dissertation, Université d'Ottawa/University of Ottawa). <https://doi.org/10.20381/ruor-31003>
17. Ajala, S. O., & Alexander, M. L. (2022). Evaluating the effects of agitation by shaking, stirring and air sparging on growth and accumulation of biochemical compounds in microalgae cells. *Biofuels*, 13(3), 371–381. <https://doi.org/10.1080/17597269.2020.1714161>
18. Kamaruzaman, D., Mustakim, N. S. M., Subki, A. S. R. A., Parimon, N., Yaakob, M. K., Malek, M. F., Vasimalai, N., Abdullah, M. H., Bakar, S. A., Ahmad, M. K., Thomas, S. & Mamat, M. H. (2024). Polystyrene waste-ZnO nanocomposite film for energy harvesting via hydrophobic triboelectric nanogenerator: Transforming waste into energy. *Materials Today Sustainability*, 26, 100726. <https://doi.org/10.1016/j.mtsust.2024.100726>
19. Zhu, Y., Liu, S., Chen, H., Yu, P., & Chen, C. (2025). Evaluating biochar for adsorption of ammonium nitrogen in wastewater: insights into modifications and mechanisms. *Environmental Research*, 121615. <https://doi.org/10.1016/j.envres.2025.121615>
20. Dehkhoda, A. M., Gyenge, E., & Ellis, N. (2016). A novel method to tailor the porous structure of KOH-activated biochar and its application in capacitive deionization and energy storage. *Biomass and Bioenergy*, 87, 107–121. <https://doi.org/10.1016/j.biombioe.2016.02.023>
21. Zhang, Y., Zhao, Y. P., Qiu, L. L., Xiao, J., Wu, F. P., Cao, J. P., ... & Liu, F. J. (2022). Insights into the KOH activation parameters in the preparation of corncob-based microporous carbon for high-performance supercapacitors. *Diamond and Related Materials*, 129, 109331. <https://doi.org/10.1016/j.diamond.2022.109331>

22. Ahmad, M., Rajapaksha, A. U., Lim, J. E., Zhang, M., Bolan, N., Mohan, D., Vithanage, M., Lee, S. S. & Ok, Y. S. (2014). Biochar as a sorbent for contaminant management in soil and water: A review. *Chemosphere*, 99, 19–23. <https://doi.org/10.1016/j.chemosphere.2013.10.071>
23. Zhu, K., Li, K., Zeng, Y., Wang, Y., Chen, Y., Zhang, Y., ... & Yan, K. (2024). Fundamentals of biomass-derived porous carbon. In *Fabrication and applications of biomass-derived porous carbon* (pp. 1-46). CRC Press. <https://doi.org/10.1201/9781003520566>
24. Skic, K., Adamczuk, A., Gryta, A., Boguta, P., Tóth, T., & Jozefaciuk, G. (2024). Surface areas and adsorption energies of biochars estimated from nitrogen and water vapour adsorption isotherms. *Scientific Reports*, 14(1), 30362. <https://doi.org/10.1038/s41598-024-81030-9>
25. Wang, Y., Chen, L., Zhu, Y., Fang, W., Tan, Y., He, Z., & Liao, H. (2024). Research status, trends, and mechanisms of biochar adsorption for wastewater treatment: A scientometric review. *Environmental Sciences Europe*, 36,-25. <https://doi.org/10.1186/s12302-024-00859-z>
26. Santos, D. C. B. D., Evaristo, R. B. W., Dutra, R. C., Suarez, P. A. Z., Silveira, E. A., & Ghesti, G. F. (2025). Advancing biochar applications: A review of production processes, analytical methods, decision criteria, and pathways for scalability and certification. *Sustainability*, 17(6), 2685. <https://doi.org/10.3390/su17062685>
27. Wang, Z., Li, J., Zhang, G., Zhi, Y., Yang, D., Lai, X., & Ren, T. (2020). Characterization of acid-aged biochar and its ammonium adsorption in an aqueous solution. *Materials*, 13(10), 2270. <https://doi.org/10.3390/ma13102270>
28. Shenk, A., Ivan, J. P. A., Schwede, S., & Odlare, M. (2022). Analysis of influencing characteristics of biochars for ammonium adsorption. *Applied Sciences*, 12(19), 9487. <https://doi.org/10.3390/app12199487>
29. Kumari, B., Tiwary, R. K., Yadav, M., & Singh, K. M. P. (2021). Nonlinear regression analysis and response surface modeling of Cr (VI) removal from synthetic wastewater by an agro-waste Cocos Nucifera: Box-Behnken Design (BBD). *International Journal of Phytoremediation*, 23(8), 791–808. <https://doi.org/10.1080/15226514.2020.1858399>
30. Agboola, O. D., & Benson, N. U. (2021). Physisorption and chemisorption mechanisms influencing micro (nano) plastics-organic chemical contaminants interactions: A review. *Frontiers in Environmental Science*, 9, 678574. <https://doi.org/10.3389/fenvs.2021.678574>
31. Yuan, J., Amano, Y. & Machida, M. Characterization of High-Performance Zinc Chloride Activated Biochar Modified by Thermal Chemical Vapor Deposition (CVD) and Its Removal Mechanism of Aqueous Nitrate Ions. *Int J Environ Res* 16, 57 (2022). <https://doi.org/10.1007/s41742-022-00430-9>
32. Chen, W., Ding, S., Lin, Z., Peng, Y., & Ni, J. (2020). Different effects of N₂-flow and air-limited pyrolysis on bamboo-derived biochars' nitrogen and phosphorus release and sorption characteristics. *Science of The Total Environment*, 711, 134828. <https://doi.org/https://doi.org/10.1016/j.scitotenv.2019.134828>
33. Fan, R., Chen, C.-l., Lin, J.-y., Tzeng, J.-h., Huang, C.-p., Dong, C., & Huang, C. P. (2019). Adsorption characteristics of ammonium ion onto hydrous biochars in dilute aqueous solutions. *Bioresource Technology*, 272, 465-472. <https://doi.org/https://doi.org/10.1016/j.biortech.2018.10.064>
34. Chen, L., Chen, X. L., Zhou, C. H., Yang, H. M., Ji, S. F., Tong, D. S., Zhong, Z. K., Yu, W. H., & Chu, M. Q. (2017). Environmental-friendly montmorillonite-biochar composites: Facile production and tunable adsorption-release of ammonium and phosphate. *Journal of Cleaner Production*, 156, 648-659. <https://doi.org/https://doi.org/10.1016/j.jclepro.2017.04.050>